International Journal of Minerals, Metallurgy and Materials
Volume 25, Number 5, May 2018, Page 564
https://doi.org/10.1007/s12613-018-1603-x

Microstructure and mechanical properties of Al/Cu/Mg laminated composite sheets produced by the ARB proces

Davood Rahmatabadi[1)], *Moslem Tayyebi*[2)], *Ramin Hashemi*[1)], *and Ghader Faraji*[3)]

1) School of Mechanical Engineering, Iran University of Science and Technology, Tehran 16846-13114, Iran
2) Department of Materials Engineering, Sahand University of Technology, Tabriz 51978-17169, Iran
3) School of Mechanical Engineering, College of Engineering, University of Tehran, Tehran 11155-4563, Iran
(Received: 14 June 2017; revised: 6 August 2017; accepted: 8 August 2017)

Abstract: In the present study, an Al/Cu/Mg multi-layered composite was produced by accumulative roll bonding (ARB) through seven passes, and its microstructure and mechanical properties were evaluated. The microstructure investigations show that plastic instability occurred in both the copper and magnesium reinforcements in the primary sandwich. In addition, a composite with a perfectly uniform distribution of copper and magnesium reinforcing layers was produced during the last pass. By increasing the number of ARB cycles, the microhardness of the layers including aluminum, copper, and magnesium was significantly increased. The ultimate tensile strength of the sandwich was enhanced continually and reached a maximum value of 355.5 MPa. This strength value was about 3.2, 2, and 2.1 times higher than the initial strength values for the aluminum, copper, and magnesium sheets, respectively. Investigation of tensile fracture surfaces during the ARB process indicated that the fracture mechanism changed to shear ductile at the seventh pass.

Keywords: multi-layered composite; Al/Cu/Mg; accumulative roll bonding; fractography; mechanical properties; microstructure

1. Introduction

Metal matrix composites (MMCs) have broad and various applications. The strength, hardness, thermal conductivity, wear resistance, creep resistance, and dimensional stability of MMCs show improvement compared to the base metal [1–2]. Aluminum (Al), due to its good engineering properties, simplicity of processing, and low density is a metal that is regarded highly in composite manufacture [3–4]. Magnesium (Mg) is a lightweight metal with a hexagonal close packed (hcp) structure and has many applications in the medical, automotive, and aerospace industries [5–7]. Copper (Cu) is also a metal and displays high electrical and thermal conductivity and excellent formability. A composite consisting of Al, Cu, and Mg, can provide a variety of properties such as high strength, light weight, and good thermal and electrical conductivity. Several methods are used for manufacturing multilayer composites. One of the top-down strategies includes severe plastic deformation (SPD) processing methods. Up to now, various SPD processes such as equal channel angular pressing (ECAP) [8–11], high pressure torsion (HPT) [8,12–14], multi-axial forging (MAF) [15], repetitive forging [16], tubular channel angular pressing (TCAP) [17–18], cyclic extrusion compression (CEC) [19–20], and accumulative roll bonding (ARB) [21–22] have been proposed as effective SPD methods and successfully applied to various materials. The common feature of these techniques is that the shape and dimension of the sample are approximately constant after processing so there is no geometric limitation when applying very high plastic strain [23]. Among these processes, ARB has some unique features, e.g.: (1) unlike the ECAP, CEC, and HPT processes which require forming machines with a large capacity and expensive dies, the ARB process can be performed by a conventional rolling mill without any particular die [23]; (2) compared with other methods, the productivity of the ARB process is relatively high because it can be potentially upscaled to an industrial level for a continuous production of ultrafine-grained metallic sheets or plates [21]. In recent years, the ARB process has been used to produce many multilayer

Corresponding author: Ramin Hashemi E-mail: rhashemi@iust.ac.ir

composites with differing and similar materials such as Al/Cu [24], Al/Zn [25], Al/Mg [26], Al/Ni [27], Cu/Ni [28], and Al/Ti [29]. Also, there has been limited research into producing MMCs with more than two different materials, i.e., Al/Ti/Mg [30], Al/Zn/Cu [31], Al/Ti/Nb [32], and Al/Ni/Cu [33].

In the present study, an Al/Cu/Mg multilayer composite was produced by the ARB process over seven passes at room temperature without lubrication. Then, its microstructure and mechanical properties were evaluated after each ARB cycle.

2. Experimental

2.1. Materials

The materials employed in this study were commercially pure Al, Cu, and AZ31B Mg alloy. Table 1 shows the chemical composition, mechanical properties, and primary dimensions of these materials.

2.2. ARB process

Fig. 1(a) shows a schematic illustration of the primary sandwich production. At first, a primary sandwich was

Table 1. Specifications of primary materials

Material	Chemical composition / wt%	Ultimate tensile strength / MPa	Micro hardness, HV	Primary dimension / mm		
				Length	Width	Thickness
Al 1050	Al 99.17, Mg 0.05, Fe 0.4, Cr 0.2, Si 0.25, Mn 0.05, Zn 0.05, Ti 0.03	110.5	34	120	50	1
Pure Cu	Cu 99.9, Fe 0.006 and other elements were balanced	179.5	74.5	120	50	1
Mg AZ31B	Mg 95.8, Al 3, Zn 1, Mn 0.2	170.35	67.3	120	50	1.5

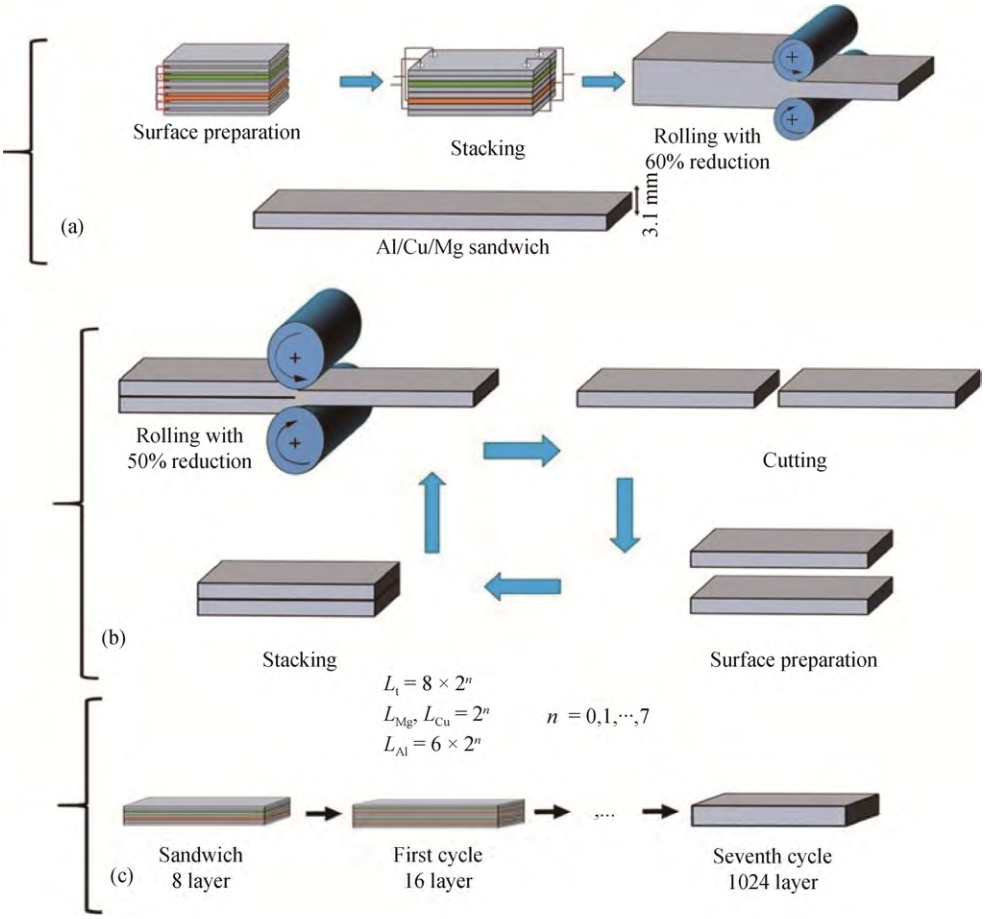

Fig. 1. Schematic illustration of ARB for producing Al/Cu/Mg multi-layered composites: (a) primary sandwich production; (b) ARB process; (c) the multiplayer composite.

fabricated, then the ARB process was performed. To fabricate the primary sandwich, six Al sheets, one Cu sheet, and one Mg sheet were prepared to the same dimensions. These were then degreased in acetone, air-dried, scratch brushed, and stacked on top of each other, as shown in Fig. 1(a). The sheets were then assembled as a sandwich stack. To prevent slippage, the stack was clamped using copper wires at the edges. Finally, to fabricate the primary sandwich, a 60% reduction in thickness was applied. The thickness of the sandwich stacks reduced from 8.5 to 3.1 mm using the rolling process at room temperature, again shown in Fig. 1(a). The real samples of the prepared stacked and the produced primary sandwich are shown in Fig. 2.

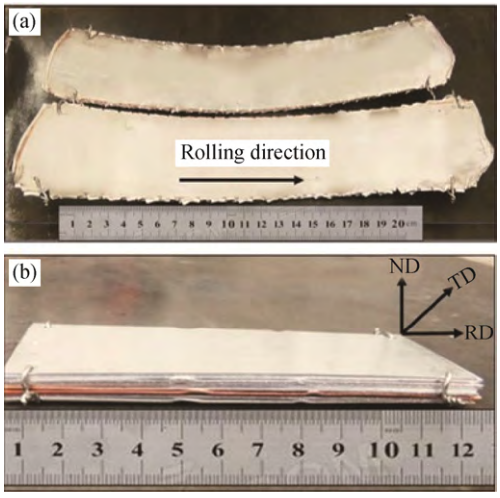

Fig. 2. The primary sandwich after (a) and before (b) rolling.

Fig. 1(b) shows a schematic illustration of the ARB process. The surface preparation was performed in multiple steps, i.e., degreased with acetone, air-dried, and roughened with a circular stainless-steel wire brush. Finally, after clamping, roll-bonded sheets with a 50% reduction in thickness were created. The ARB process was repeated for seven cycles. The process was performed using a laboratory rolling mill with a 107 mm roller diameter at room temperature, with no lubricant. After the seventh pass, a multilayer composite with 1024 layers was produced (Fig. 1(c)).

2.3. Microstructure

The microstructure of the processed specimens after different ARB cycles was evaluated using optical microscopy. After each pass, specimens were cut using wire cut electro discharge machining parallel to the rolling direction. Then, they were ground using sandpaper, number 100 to 5000, and polished using a mixture of alumina powder with a particle size of 0.3 μm, water, and soap. Finally, polishing with alcohol and alumina, without water, was carried out to remove the magnesium oxide layers. After the uniaxial tensile tests, the tensile fracture surfaces were viewed using a scanning electron microscope (model VEGA TESCAN). X-ray diffraction (XRD) measurements were carried out on the RD–TD plane of the ARB processed sheets. The XRD experiments were performed using an X-ray diffractometer (XRD, Bruker Advance D8) with Cu K_α radiation (λ = 0.15406 nm). The X-ray was operated at 40 kV, 0.5°, and 40 mA and the data were collected at room temperature with a 2θ range between 30° and 90°. The Williamson–Hall formula and X´Pert High Score software were used to analyze the XRD data.

2.4. Mechanical properties

The mechanical properties of the Al/Cu/Mg multi-layered composite fabricated by the ARB process were investigated using uniaxial tensile tests and microhardness measurements. Uniaxial tensile test samples were prepared from the unprocessed and ARB processed sheets oriented along the rolling direction, according to the JISZ2201 standard. The gage length and width of the tensile test specimens were 11.6 and 3 mm, respectively. The uniaxial tensile tests were performed at an initial strain rate of 0.5 mm/min at room temperature using a SANTAM tensile testing machine. Vickers microhardness tests were performed on the initial and ARB samples using a JENUS apparatus under a load of 1.96 N applied for 10 s. Microhardness tests were performed on the Al, Cu, and Mg layers randomly at ten different points on cross-sections perpendicular to the rolling direction. Then, for each Al, Cu, and Mg layer the minimum and maximum hardness values were disregarded.

3. Results and discussion

3.1. Microstructure

Fig. 3 illustrates the microstructure of the Al/Cu/Mg multi-layered composite after the ARB process. The difference in the flow properties of the metal matrix and reinforcing caused plastic instability (fracture and necking) during ARB processing [30–31]. When the applied strain was increased, plastic instability was observed in the Cu and Mg layers, as shown in Figs. 3(a) and 3(c). The copper layers in an Al matrix were continuous and coherent at the end of the first cycle, but plastic instability was observed in the Mg layers of the primary sandwich. Due to the high formability and work hardening of Al compared with both reinforcing layers (Cu and Mg), large plastic strain was applied to the Al and a large reduction in thickness was observed in its layers with significant work hardening. However, the reinforcing layers deformed more than the Al layers and, inevitably, showed

plastic instability. Previous investigations have reported that reinforcing distribution is non-uniform in early ARB passes due to non-uniform strain. This is a result of friction between the roller and the sample, and also between the layers due to the differences in flow properties [24,30,34]. By increasing the number of ARB cycles, the difference in the flow properties between the matrix (Al) and reinforcement (Cu and Mg) reduced. This led to the production of a multi-layered composite with a uniform distribution of both Cu and Mg layers within the Al matrix (Fig. 3(h)).

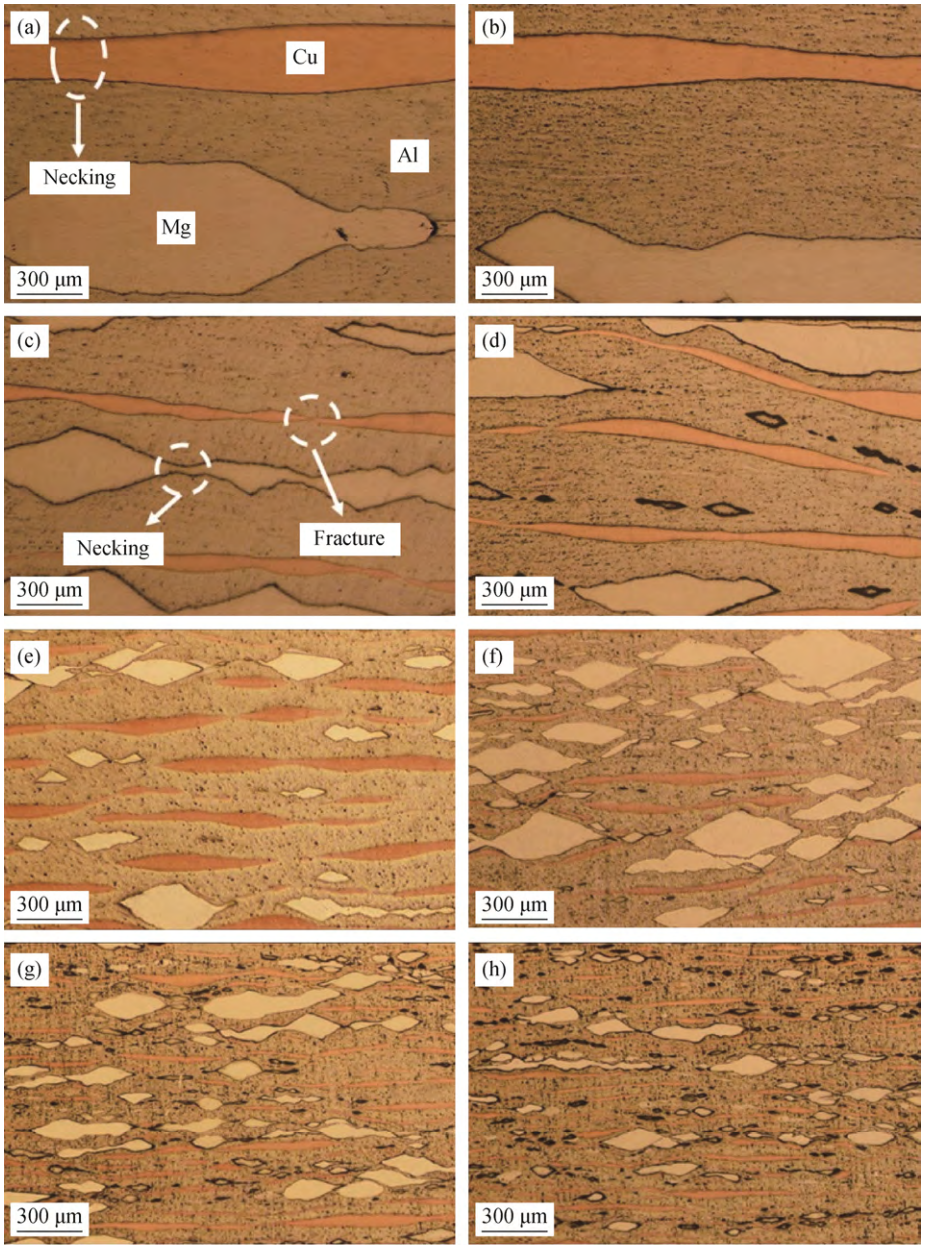

Fig. 3. Microstructure of the ARB processed Al/Cu/Mg multi-layered composite: (a) primary sandwich; (b) after the first cycle; (c) after the second cycle; (d) after the third cycle; (e) after the fourth cycle; (f) after the fifth cycle; (g) after the sixth cycle; (h) after the seventh cycle.

Fig. 4 shows the thickness variations in both the Cu and Mg reinforcing layers at the different passes of the ARBed Al/Cu/Mg composite. Because of the high applied strain, the thickness of the Cu and Mg layers during the early ARB passes decreased sharply. Then, the thickness of the Cu and Mg layers reduced at a lower rate because of layer fracturing, which reduced formability [24,30,34]. The highest rate of thickness reduction of the Mg and Cu layers occurred at the first and second pass, respectively. Finally, the 1000 and 1500 μm initial sample thicknesses of the Cu and Mg layers

were reduced to approximately 18 and 30 μm, respectively, after the seventh cycle of the ARB process.

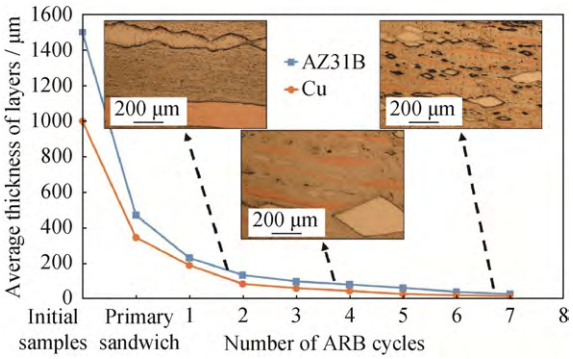

Fig. 4. Thickness variations in the copper and magnesium layers of the processed Al/Cu/Mg composite after different numbers of ARB cycles.

Fig. 5 shows the typical XRD patterns of the Al/Cu/Mg composite after the primary sandwich and seventh ARB cycle. XRD analysis showed that by increasing the number of ARB cycles, no new peak was added to previous peaks, which shows that no new phase or new combination was produced. This phenomenon was predictable as the composite fabrication was performed at room temperature. Also, due to the low strain rates and relatively low speed of the rolling mill, not much heat was created and this was less than the activation energy necessary to produce intermetallic compounds [35]. Crystallite size in the Al matrix after primary sandwich rolling and seventh ARB cycle was 208 and 132 nm, respectively. Deformation mechanisms in the microstructure of multi-phase materials present strong obstacles to the movement of dislocations because of different interfaces between the phases [36]. According to conducted research on the ARB process, the structural changes and

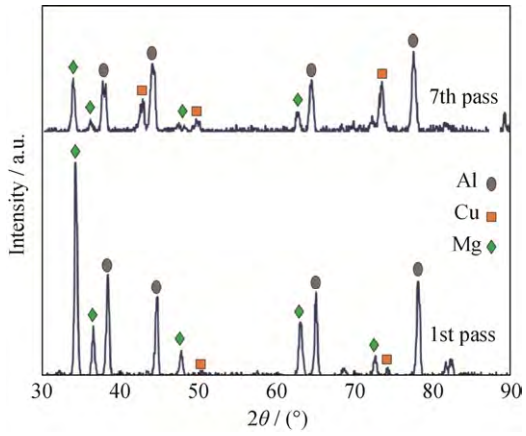

Fig. 5. XRD pattern of the nanostructured Al/Cu/Mg metallic multilayer composite after the primary sandwich and seventh ARB cycle.

creation of ultrafine grains are independent of the type of metal and the average grain size of each material is different [22]. These differences could be attributed to stacking fault energy, processing temperature, strain rate, and so on. During SPD at low temperatures, boundary areas with a high deviation angle were created by two mechanisms: (a) expansion borders that existed in the material from the beginning and (b) the production of new high-angle boundaries [37–38].

3.2. Mechanical properties

Fig. 6 illustrates the microhardness variations in the individual Cu, Mg, and Al layers at various ARB passes. It is apparent that by increasing the number of ARB passes, the microhardness of all the layers (Cu, Mg, and Al) increased. The microhardness values of the Cu, Al, and Mg layers after the first pass increased about 1.86, 1.77, and 1.6 times, respectively, compared with the initial samples. Accordingly, the sharp rise in microhardness during the early ARB cycles could be attributed to work hardening, dislocation density increase, and the formation of new subgrain boundaries [24–25,33,39]. Increasing the number of ARB passes from two to five led to an increase in the microhardness of all layers although the rate of increase was less than during early cycles. This may be because work hardening and grain refinement are greater during the early cycles of SPD processing [40–41]. At the intermediate passes, the rate of work hardening was less than at the initial passes [4,33]. Finally, from the fifth to the seventh passes, the microhardness reached a saturated value resulting from a saturation in grain size. At the last pass, the microhardness of the Al, Cu, and Mg layers reached HV 77.4, HV 146.1, and HV 121.5, respectively. Compared with the initial samples, the microhardness of the Al, Cu, and Mg layers increased 2.15, 1.96 and 1.80 times, respectively. The main reason for the increasing microhardness was grain refinement [24–25,33,39].

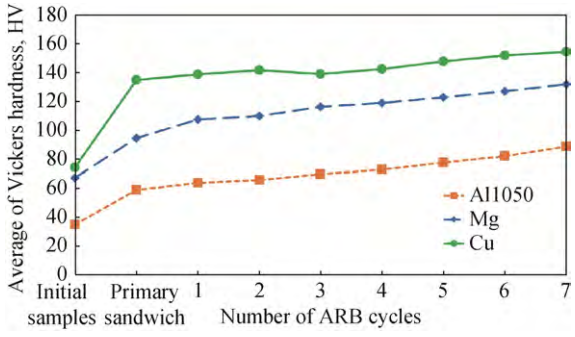

Fig. 6. Microhardness variations in aluminum, copper, and magnesium layers after different numbers of ARB cycles.

The engineering stress–strain curves of the initial unprocessed strips are shown in Fig. 7 and those of the multilayer composite Al/Cu/Mg after the ARB process are shown in Fig. 8. When increasing the number of ARB cycles, the strength increased and the elongation decreased at first, then the elongation increased. Fig. 9 shows the variation in tensile strength and elongation of the multilayer composite Al/Cu/Mg processed by ARB through different cycles. Tensile strength increased continuously up to the seventh cycle. The maximum tensile strength was achieved after the last cycle of the ARB process and reached 355.5 MPa. This strength value was 3.2, 2, and 2.1 times higher than that of the initial Al, Cu, and Mg sheets, respectively. Also, from the primary sandwich, the elongation decreased and then increased continuously up to seventh cycle. Researchers have reported several major factors including work hardening, grain refinement, particle shape, type and size, amount of applied deformation, quality of bonding layers, and distribution of reinforcement [4,25,33,39,42] that could cause changes in the tensile strength of MMCs. During the early ARB passes, strengthening is mainly due to work hardening, the formation of low angle subgrain boundaries, and an increase in the density of dislocations [4,24,25,33,43]. Subsequently, the strengthening mechanism is mainly due to grain refinement. During the last cycle of ARB process, the strength value increased due to the fine-grained microstructure and distribution of the Cu reinforcement.

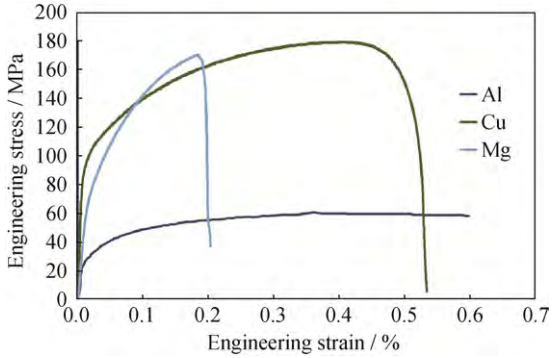

Fig. 7. Engineering stress–strain curves of the primary materials.

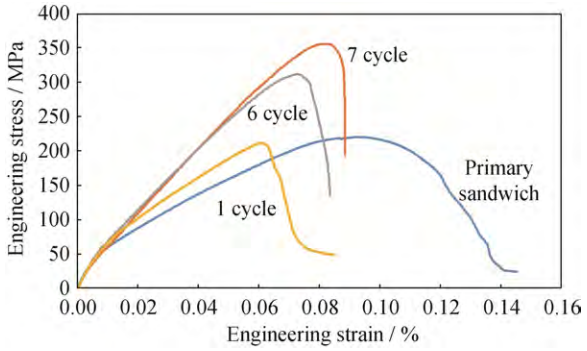

Fig. 8. Engineering stress–strain curves of the ARB processed Al/Cu/Mg composite.

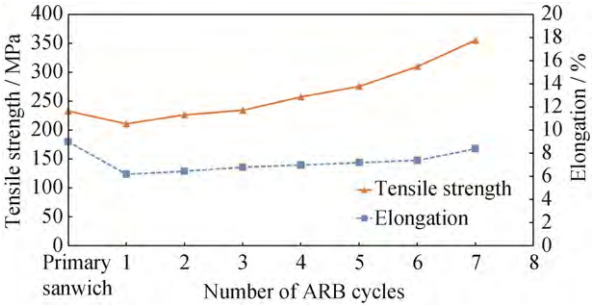

Fig. 9. Variations in tensile strength and elongation of the Al/Cu/Mg composite after different numbers of ARB cycles.

Table 2 shows a comparison of the strength and ductility of the multi-layered Al/Cu/Mg composite produced in the present study with those from previous works. It can be concluded from Table 2 that elongation of the composite without particle reinforcement was greater than that with because the strength of the powder/metal interface was weaker. The powder/metal interface is a good place for the germination of cracks and defects leading to fracture initiation. It can also be understood that using a two-phase hcp structure caused further reduction in elongation. Also, higher ductility was obtained from the Al/Cu/Mg ARB processed composite than in previous studies. The reason for this was probably due to grain refinement and a higher bond strength between the layers, which was higher than in most previous studies and included Al/Ti/Mg, Al/Cu/Ni, Al/Cu/Mn, Al/Cu/Al_2O_3, and Al/Cu.

Table 2. Comparison of the strength and ductility values of the multi-layered composite in present study with those from previous works

Materials	Maximum value of ultimate tensile strength / MPa	Maximum value of elongation / %	ARB cycle	Reference
Al/Cu/Mg	355.5	8.40	7	This study
Al/Ti/Mg	335.9	2.30	4	[30]
Al/Cu/Ni	346	7.80	11	[33]
Al/Cu/Zn	290	15.00	4	[31]
Al/Cu/Mn	355	6.90	9	[4]
Al/Cu/Al_2O_3	361	5.00	7	[42]
Al/Cu	365	7.93	5	[24]
Al/Cu	385.5	7.30	7	[44]

3.3. Fractography

Fig. 10 illustrates the tensile fracture surfaces of the Cu and Mg sheets after uniaxial tensile testing. The basic fracture mechanisms of Al, Cu, and Mg were ductile, ductile, and brittle fracture, respectively. The basic fracture mechanisms of the most coarse-grained metals with face centered cubic (fcc) and hexagonal centered cubic (hcp) crystal structures were ductile and brittle, respectively [30]. Fig. 11

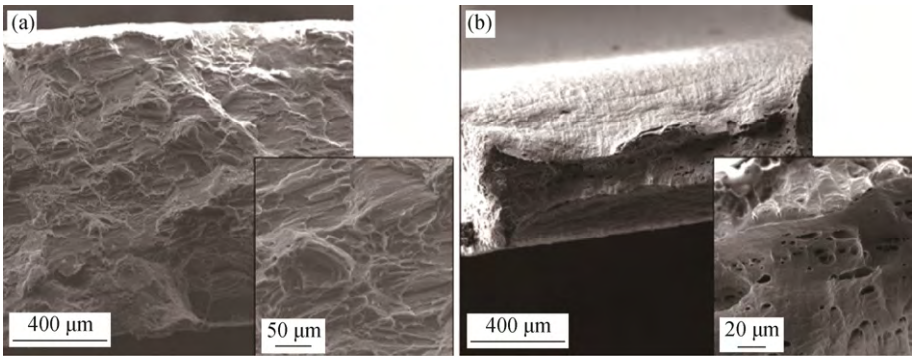

Fig. 10. Tensile fracture surfaces of the initial sheets before the ARB process: (a) Mg; (b) Cu.

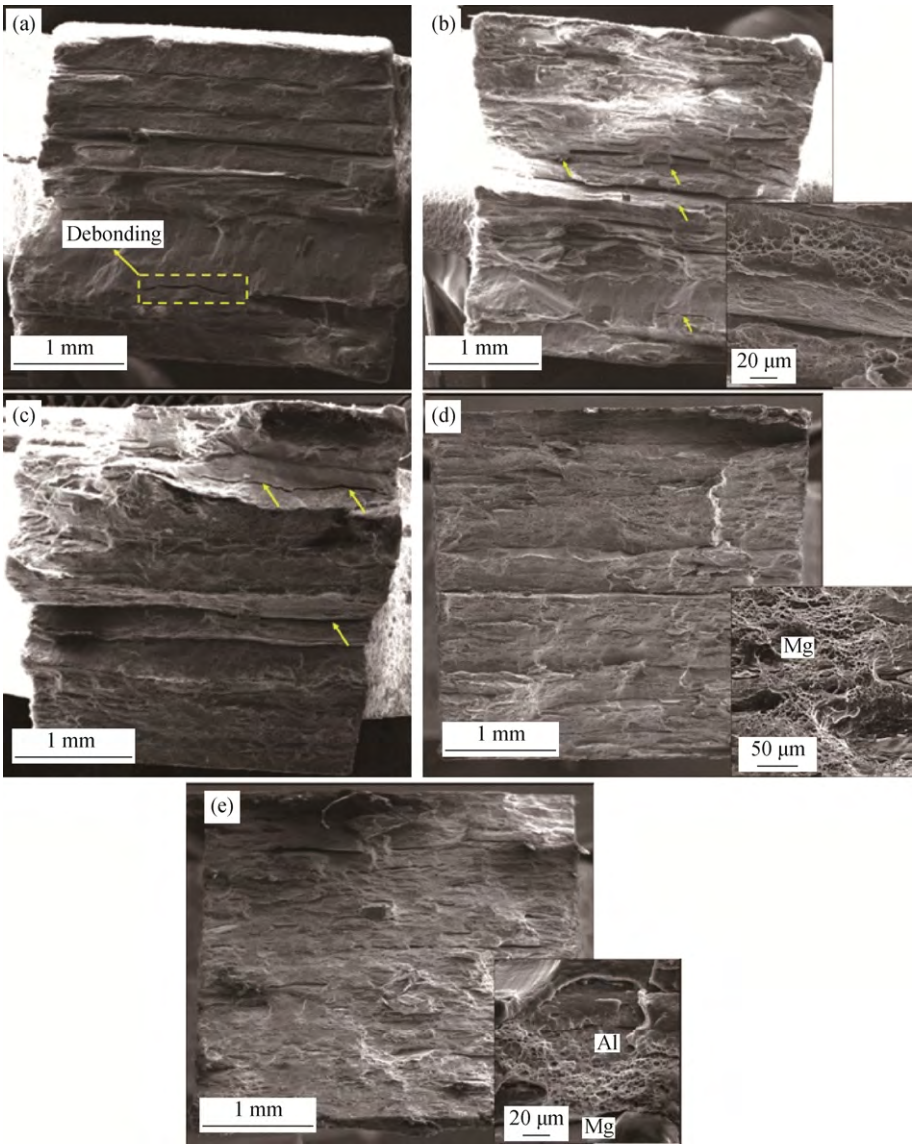

Fig. 11. Tensile fracture surfaces of the Al/Cu/Mg multi-layered composite: (a) primary sandwich; (b) after the first cycle; (c) after the second cycle; (d) after the third cycle; (e) after the fourth cycle.

shows the tensile fracture surfaces of the Al/Cu/Mg multi-layered composite in the Al, Cu, and Mg layers after the primary sandwich. Debonding can be seen between the Al/Mg interfaces in the primary sandwich. Also, a lamellar structure exhibited up to the fourth cycle, see Fig. 11(c). By increasing the number of ARB cycles, bonding between the layers became stronger and the lamellar structure decreased, though it still existed even after the sixth and seventh cycles [42]. It can also be seen that the fracture surfaces at the seventh pass exhibit a shear ductile mode [30].

4. Conclusions

(1) Plastic instability was observed in the Mg and Cu layers of the primary sandwich and during the second cycle.

(2) The Cu and Mg layers were reduced in thickness from initial values of 1000 and 1500 μm to approximately 18 and 30 μm, respectively, after the seventh ARB cycle.

(3) By increasing the number of ARB cycles to seven, a multi-layered composite with 1024 layers and uniform Cu and Mg distribution was produced.

(4) By increasing the number of ARB cycles, the microhardness of the three Al, Cu, and Mg layers was increased.

(5) The tensile strength of the sandwich was enhanced continually and a maximum value of 355.5 MPa was achieved.

(6) The tensile fracture surfaces of the produced composite from the second to the fourth pass displayed a lamellar structure, and depending on the interfaces, the fracture mechanism for Al finally changed to shear ductile.

References

[1] F.A. Marandi, A.H. Jabbari, M. Sedighi, and R. Hashemi, An Experimental, analytical, and numerical investigation of hydraulic bulge test in two-layer Al–Cu Sheets, *J. Manuf. Sci. Eng.*, 139(2017), No. 3, article No. 031005.

[2] M.H. Vini, M. Sedighi, and M. Mondali, Mechanical properties, bond strength and microstructural evolution of AA1060/TiO_2 composites fabricated by warm accumulative roll bonding (WARB), *Int. J. Mater. Res.*, 108(2017), No. 1, p. 53.

[3] H. Rahimi, M. Sedighi, and R. Hashemi, Forming limit diagrams of fine-grained Al 5083 produced by equal channel angular rolling process, [in] *Proceedings of the Institution of Mechanical Engineers, Part L. Journal of Materials: Design and Applications*, 2016. https://doi.org/10.1177/1464420716655560.

[4] M. Alizadeh and M. Samiei, Fabrication of nanostructured Al/Cu/Mn metallic multilayer composites by accumulative roll bonding process and investigation of their mechanical properties, *Mater. Des.*, 56(2014), p. 680.

[5] K. Wu, H. Chang, E. Maawad, W.M. Gan, H.G. Brokmeier, and M.Y. Zheng, Microstructure and mechanical properties of the Mg/Al laminated composite fabricated by accumulative roll bonding (ARB), *Mater. Sci. Eng. A*, 527(2010), No. 13-14, p. 3073.

[6] P. Asadi, G. Faraji, and M.K. Besharati, Producing of AZ91/SiC composite by friction stir processing (FSP), *Int. J. Adv. Manuf. Technol.*, 51(2010), No. 1-4, p. 247.

[7] G. Faraji, O. Dastani, and S.A.A.A. Mousavi, Effect of process parameters on microstructure and micro-hardness of AZ91/Al_2O_3 surface composite produced by FSP, *J. Mater. Eng. Perform.*, 20(2011), No. 9, p. 1583.

[8] R.Z. Valiev, R.K. Islamgaliev, and I.V. Alexandrov, Bulk nanostructured materials from severe plastic deformation, *Prog. Mater. Sci.*, 45(2000), No. 2, p. 103.

[9] R.Z. Valiev and T.G. Langdon, Principles of equal-channel angular pressing as a processing tool for grain refinement, *Prog. Mater. Sci.*, 51(2006), No. 7, p. 881.

[10] R.Z. Valiev, N.A. Krasilnikov, and N.K. Tsenev, Plastic deformation of alloys with submicron-grained structure, *Mater. Sci. Eng. A*, 137(1991), p. 35.

[11] A. Azimi, S. Tutunchilar, G. Faraji, and M. B. Givi, Mechanical properties and microstructural evolution during multi-pass ECAR of Al 1100-O alloy, *Mater. Des.*, 42(2012), p. 388.

[12] G. Sakai, Z. Horita, and T. G. Langdon, Grain refinement and superplasticity in an aluminum alloy processed by high-pressure torsion, *Mater. Sci. Eng. A*, 393(2004), No. 1-2, p. 344.

[13] A.P. Zhilyaev and T.G. Langdon, Using high-pressure torsion for metal processing: Fundamentals and applications, *Prog. Mater. Sci.*, 53(2008), No. 6, p. 893.

[14] Z.J. Horita, D.J. Smith, M. Furukawa, M. Nemoto, R.Z. Valiev, and T.G. Langdon, An investigation of grain boundaries in submicrometer-grained Al–Mg solid solution alloys using high-resolution electron microscopy, *J. Mater. Res.*, 11(1996), No. 8, p. 1880.

[15] J.G. Yin, J. Lu, H.T. Ma, and P.S. Zhang, Nanostructural formation of fine grained aluminum alloy by severe plastic deformation at cryogenic temperature, *J. Mater. Sci.*, 39(2004), No. 8, p. 2851.

[16] A. Babaei, G. Faraji, M.M. Mashhadi, and M. Hamdi, Repetitive forging (RF) using inclined punches as a new bulk severe plastic deformation method, *Mater. Sci. Eng. A*, 558(2012), p. 150.

[17] G. Faraji, K. Abrinia, M.M. Mashhadi, and M. Hamdi, An upper-bound analysis for frictionless TCAP process, *Arch. Appl. Mech.*, 83(2013), No. 4, p. 483.

[18] G. Faraji, M.M. Mashhadi, and H.S. Kim, Tubular channel angular pressing (TCAP) as a novel severe plastic deformation method for cylindrical tubes, *Mater. Lett.*, 65(2001), No. 19-20, p. 3009.

[19] M. Richert, H. Stüwe, J. Richert, R. Pippan, and C. Motz, Characteristic features of microstructure of AlMg5 deformed to large plastic strains, *Mater. Sci. Eng. A*, 301(2001), No. 2,

p. 237.
[20] J. Richert and M. Richert, A new method for unlimited deformation of metals and alloys, *Aluminum*, 62(1986), No. 8, p. 604.
[21] Y. Saito, H. Utsunomiya, N. Tsuji, and T. Sakai, Novel ultra-high straining process for bulk materials-development of the accumulative roll-bonding (ARB) process, *Acta Mater*., 47(1999), No. 2, p. 579.
[22] Y. Saito, R.G. Hong, N. Tsuji, H. Utsunomiya, and T. Sakai, Ultra-fine grained bulk aluminum produced by accumulative roll-bonding (ARB) process, *Scripta Mater*., 39(1998), No. 9, p. 1221.
[23] H. Pirgazi, A. Akbarzadeh, R. Petrov, and L. Kestens, Microstructure evolution and mechanical properties of AA1100 aluminum sheet processed by accumulative roll bonding, *Mater. Sci. Eng. A*, 497(2008), No. 1-2, p. 132.
[24] M. Eizadjou, A.K. Talachi, H.D. Manesh, H.S. Shahabi, and K. Janghorban, Investigation of structure and mechanical properties of multi-layered Al/Cu composite produced by accumulative roll bonding (ARB) process, *Compos. Sci. Technol.*, 68(2008), No. 9, p. 2003.
[25] R.N. Dehsorkhi, F. Qods, and M. Tajally, Investigation on microstructure and mechanical properties of Al–Zn composite during accumulative roll bonding (ARB) process, *Mater. Sci. Eng. A*, 530(2011), p. 63.
[26] H. Chang, M.Y. Zheng, C. Xu, G.D. Fan, H.G. Brokmeier, and K. Wu, Microstructure and mechanical properties of the Mg/Al multilayer fabricated by accumulative roll bonding (ARB) at ambient temperature, *Mater. Sci. Eng. A*, 543(2012), p. 249.
[27] A. Mozaffari, H.D. Manesh, and K. Janghorban, Evaluation of mechanical properties and structure of multilayered Al/Ni composites produced by accumulative roll bonding (ARB) process, *J. Alloys Compd.*, 489(2010), No. 1, p. 103.
[28] M. Tayyebi and B. Eghbali, Study on the microstructure and mechanical properties of multilayer Cu/Ni composite processed by accumulative roll bonding, *Mater. Sci. Eng. A*, 559(2013), p. 759.
[29] H.P. Ng, T. Przybilla, C. Schmidt, R. Lapovok, D. Orlov, H.W. Hppel, and M. Gken, Asymmetric accumulative roll bonding of aluminium-titanium composite sheets, *Mater. Sci. Eng. A*, 576(2013), p. 306.
[30] P.D. Motevalli and B. Eghbali, Microstructure and mechanical properties of Tri-metal Al/Ti/Mg laminated composite processed by accumulative roll bonding, *Mater. Sci. Eng. A*, 628(2015), p. 135.
[31] M.M. Mahdavian, L. Ghalandari, and M. Reihanian, Accumulative roll bonding of multilayered Cu/Zn/Al: An evaluation of microstructure and mechanical properties, *Mater. Sci. Eng. A*, 579(2013), p. 99.
[32] R. Zhang and V.L. Acoff, Processing sheet materials by accumulative roll bonding and reaction annealing from Ti/Al/Nb elemental foils, *Mater. Sci. Eng. A*, 463(2007), No. 1-2, p. 67.
[33] A. Shabani, M.R. Toroghinejad, and A. Shafyei, Fabrication of Al/Ni/Cu composite by accumulative roll bonding and electroplating processes and investigation of its microstructure and mechanical properties, *Mater. Sci. Eng. A*, 558(2012), p. 386.
[34] G. Min, J.M. Lee, S.B. Kang, and H.W. Kim, Evolution of microstructure for multilayered Al/Ni composites by accumulative roll bonding process, *Mater. Lett.*, 60(2006), No. 27, p. 3255.
[35] D. Rahmatabadi, R. Hashemi, B. Mohammadi, and T. Shojaee, Experimental evaluation of the plane stress fracture toughness for ultra-fine grained aluminum specimens prepared by accumulative roll bonding process, *Mater. Sci. Eng. A*, 708(2017), p. 301.
[36] A. Pineau, A.A. Benzerga, and T. Pardoen, Failure of metals III: Fracture and fatigue of nanostructured metallic materials, *Acta Mater.*, 107(2016), p. 508.
[37] Z.P. Xing, S.B. Kang, and H.W. Kim, Structure and properties of AA3003 alloy produced by accumulative roll bonding process, *J. Mater. Sci.*, 37(2002), No. 4, p. 717.
[38] N. Hansen, X. Huang, R. Ueji, and N. Tsuji, Structure and strength after large strain deformation, *Mater. Sci. Eng. A*, 387-389(2004), p. 191.
[39] D. Rahmatabadi and R. Hashemi, Experimental evaluation of forming limit diagram and mechanical properties of nano/ultra-fine grained aluminum strips fabricated by accumulative roll bonding, *Int. J. Mater. Res.*, 108(2017), No.12, p. 1036.
[40] H. Abdolvand, G. Faraji, M.K.B. Givi, R. Hashemi, and M. Riazat, Evaluation of the microstructure and mechanical properties of the ultrafine grained thin-walled tubes processed by severe plastic deformation, *Met. Mater. Int.*, 21(2015), No. 6, p. 1068.
[41] G. Faraji, M.M. Mashhadi, A.R. Bushroa, and A. Babaei, TEM analysis and determination of dislocation densities in nanostructured copper tube produced via parallel tubular channel angular pressing process, *Mater. Sci. Eng. A*, 563(2013), p. 193.
[42] V.Y. Mehr, A. Rezaeian, and M.R. Toroghinejad, Application of accumulative roll bonding and anodizing process to produce Al–Cu–Al_2O_3 composite, *Mater. Des.*, 70(2015), p. 53.
[43] M. Sedighi, M.H. Vini, and P. Farhadipour, Effect of alumina content on the mechanical properties of AA5083/Al_2O_3 composites fabricated by warm accumulative roll bonding, *Powder Metall. Met. Ceram.*, 55(2016), No. 7-8, p. 413.
[44] V.Y. Mehr, M.R. Toroghinejad, and A. Rezaeian, Mechanical properties and microstructure evolutions of multilayered Al Cu composites produced by accumulative roll bonding process and subsequent annealing, *Mater. Sci. Eng. A*, 601(2014), p. 40.